

Structure and properties of ZrN coatings deposited by high power impulse magnetron sputtering technology

PURANDARE, Yashodhan <<http://orcid.org/0000-0002-7544-9027>>, EHIASARIAN, Arutiun <<http://orcid.org/0000-0001-6080-3946>> and HOVSEPIAN, Papken <<http://orcid.org/0000-0002-1047-0407>>

Available from Sheffield Hallam University Research Archive (SHURA) at:

<https://shura.shu.ac.uk/3748/>

This document is the Accepted Version [AM]

Citation:

PURANDARE, Yashodhan, EHIASARIAN, Arutiun and HOVSEPIAN, Papken (2011). Structure and properties of ZrN coatings deposited by high power impulse magnetron sputtering technology. *Journal of Vacuum Science and Technology A: Vacuum, Surfaces, and Films*, 29 (1), 011004. [Article]

Copyright and re-use policy

See <http://shura.shu.ac.uk/information.html>

**Structure and properties of ZrN coatings deposited by
High Power Impulse Magnetron Sputtering (HIPIMS) technology**

Y. P. Purandare*^{a)}, A. P. Ehiasarian^{a)} and P. Eh Hovsepian^{a)}

^{a)} Nanotechnology Centre for PVD Research, Materials and Engineering Research
Institute, Sheffield Hallam University, UK S1 1WB.

*Corresponding author: Phone: +44-114-225 3469, Fax: +44-114-225-3501.

*Email: Y.Purandare@shu.ac.uk.

Abstract

Monolayer ZrN coatings were deposited exclusively by the novel High Power Impulse Magnetron Sputtering (HIPIMS) technology in an industrial scale PVD machine (HTC-1000-4 target system). Coatings were deposited on 1 micron polished M2 High speed steel, 304 L Stainless steel and on Si (100) specimens. Prior to deposition, HIPIMS plasma sustained on a Zirconium (Zr) target was utilised to pretreat the specimens.

Coatings were deposited at 400°C in a mixed N₂ and Ar atmosphere using 2 magnetrons in HIPIMS mode and at three different substrate bias voltages (U_{BIAS}) keeping all other process parameters constant. The thicknesses of the coatings measured by the ball cratering technique were in the range of 1.84 μm, 1.96 μm and 2.13 μm at bias voltages of -95 V, -75 V and -65 volts respectively, where the difference in thickness can be attributed to the re-sputtering effect. X-ray diffraction experiments on SS specimens revealed a dominating 111 texture for all three coatings irrespective of the bias voltage.

Cross-sectional transmission electron microscopy revealed extremely dense coating structures at all bias voltages, similar to the transition zone structure (Zone T) reported by Thornton. The -95 bias voltage coatings appeared extremely smooth on the top and with no dome shaped structures often associated with low ion bombardment during deposition. HIPIMS pretreatment lead to high adhesion (L_C) of the coatings to the substrate. A continuous ductile perforation of the coating was observed at progressive loads greater than 65 N however no spallation of the coating was observed up to loads of 100 N. High values of hardness (40.4 GPa), Young's Modulus (424 GPa) and compressive stress (10 GPa) were recorded for coatings deposited at -95 BV. Hardness and internal stress of the coating was found increasing with more negative bias voltages. All the coatings exhibited high dry sliding wear resistance (K_C) in the range of $6 \times 10^{-15} \text{ m}^3\text{N}^{-1}\text{m}^{-1}$. Cross-sectional Transmission Electron Microscopy and Atomic Force Microscopy analysis has been used to study the effect of ion bombardment obtained from HIPIMS on the structure of the coatings.

Keywords: Zirconium nitride, HIPIMS, ion bombardment, adhesion, texture, microstructure, bias voltage.

1. Introduction:

Zirconium nitride PVD coatings have found numerous applications in the field of wear and corrosion resistant coatings and also in applications where aesthetic appeal is of equal importance. The performance of a ZrN coating in harsh environments will be largely influenced by factors such as its adhesion to the substrates, extent of growth defects, microstructure, and most importantly coating density. The coating density and some growth defects in turn can be controlled by energising the deposition flux; which can be achieved either by: a) increasing the ionisation of the depositing flux b) application of suitable substrate bias voltages to achieve bombardment of the depositing species with the incoming ionised flux. ZrN, like most transition nitrides has been successfully deposited by sputtering and arc evaporation techniques [1-2]. It is well known that sputtering suffers from insufficient ionisation of the deposition species [3]. Plasmas by arc evaporation techniques can have a high ionised flux with multiple charge state ions [4]; however suffer from macroparticle droplet defects which compromise the quality of the coating to a large extent [5].

High Power Impulse Magnetron Sputtering (HIPIMS) provides an intermediate solution to the above problems. HIPIMS plasma is free of macroparticle generation and has a high degree of ionisation of the depositing species itself thus eliminating a need of any external ionisation device [6-7].

The current work focuses on the deposition of ZrN with the novel HIPIMS technology. The effect of ion bombardment on the microstructure and texture of the coating and in turn on the properties has been studied by varying the substrate bias voltages (U_{BIAS}) whereas other deposition parameters were maintained constant. The results have been

supported with cross-sectional transmission electron microscopy (TEM) and Atomic Force Microscopy (AFM).

2. Experiments:

2.1 Coating deposition:

In the current work test coupons of High Speed Steel (HSS), 304L Stainless steel (SS) and Si (001) wafers have been coated. The substrates were cleaned in an automated industrial cleaning line consisting of series of alkali solutions and de-ionised water tanks followed by vacuum drying. Following cleaning, the substrates were coated in an industrial sized machine HTC 1000-4, 4 target system (Hauzer Techno Coatings, Europe B.V., Venlo, The Netherlands). This machine is equipped with two HIPIMS power supplies (Hüttinger Electronic Sp. z o.o., Warsaw, Poland) which enable it to operate in either HIPIMS or Unbalanced Magnetron Sputtering (UBM) mode. For the current set of studies, coatings were deposited using two magnetrons running exclusively in HIPIMS mode. Figure 1 shows the schematic of the machine and the arrangements inside the chamber. Substrates were placed on a centrally located substrate table in one fold rotation so that they face a pair of operating magnetrons (in this case targets 1 and 3) facing each other and placed perpendicular to the other non-operating pair.

The deposition chamber was evacuated to the base pressure of 10^{-5} torr. The substrates were then subjected through a pre-treatment step where HIPIMS plasma sustained in Ar

atmosphere on one of the Zr targets was utilised to clean them on an atomic scale. The specimens were then coated with monolithic ZrN in a mixed $N_2 + Ar$ atmosphere and at a temperature of $400^\circ C$. To understand the effect of low energy ion bombardment available with HIPIMS, coatings were deposited with 3 different bias voltages of -95 V, -75 V and -65 V keeping all the other deposition parameters same.

2.2 Coating characterisation:

The coating was extensively characterised by various analytical techniques:

1. The preferred orientation of the texture and residual stress in the coatings were determined by the glancing angle technique with the Bragg-Brentano (2θ , $20-130^\circ$) geometry in a PHILIPS XPERT XRD machine.
2. A CSM nanoindenter was used to measure hardness and Young's modulus of the coating.
3. Coating adhesion (critical load (L_{C2}) of coating-substrate system failure) was measured with CSEM REVETEST under progressive loading conditions. The normal load was progressively increased from 5N to 100N at the rate of $0.01Nm^{-1}$ ($10Nmm^{-1}$) with an indenter moving at a velocity of 10 mm per minute.
4. Tribological properties of the coating were examined by subjecting the coated HSS specimens to dry sliding wear experiments at the ambient temperature. Sliding wear coefficients (K_c) and friction coefficient were measured with a pin on disk apparatus (CSM TRIBOMETER). The counterpart consisted of a 6 mm

Al₂O₃ ball and a constant normal load of 5 N was applied on the specimens which were sliding at a linear speed of 0.1 ms⁻¹ for 3760 m (60,000 laps). Dektak-150 stylus profiler was used to measure the wear scars and topographical features of the coating.

5. Microstructure of the coating was studied using cross-sectional Transmission Electron Microscopy (TEM) (Phillips CM 430,) and Scanning Electron Microscopy (SEM) (FEI NOVA-NANOSEM 200) studies. 3-D topographical features of the as deposited coating surface were also obtained using a CSM Atomic Force Microscope (AFM). An Electron Probe Micro Analyser (EPMA) based at Freiberg University, Germany was utilised to analyse the chemical composition of the coatings.
6. A spectrophotometer (MINOLTA-CM-508d) with an incident angle of 10° and a D 65 illuminant was used to measure the colour of the ZrN coatings according to the L*a*b* standard colour system.

3. Results and discussions:

3.1: Characterisation results:

Prior to coating deposition the substrates were pretreated with HIPIMS plasma sustained on a Zr target in Ar atmosphere to clean the substrates on an atomic scale. Figure 2(a) shows the bright field (BF) TEM image of a cross-section of the coating–substrate interface of the specimen deposited at U_{BIAS} = -95 V. The interface is very sharp, flat and free from droplet defects. Immediately adjacent to the interface is a

region with homogeneous dark contrast extending along the full span of the view. This signifies that nucleation grains have similar orientation along the entire interface and is evidence of epitaxial growth. This homogeneous contrast extends further at greater thicknesses of the coating. The changes in contrast (dark layer adjacent to the substrate) with film thickness are attributed to a bend sample causing diffraction contrast bend contours to appear [8]. This phenomenon of dark contrast due to bending was not visible in the cross-sections of the coatings deposited with different bias voltages, figure 5, suggesting it has no bearing on the adhesion values. Overall the coating grains exhibit a highly aligned / single crystal crystalline structure which results in extremely high adhesion values (L_{C2}) (table 1). Under progressive loading conditions all the coatings exhibited ductile perforation above loads of 65N however no spallation was observed until the load reached 100 N as visible in the Back Scattered SEM image in figure 2(b). Thus pre-treatment step utilising HIPIMS lead to high adhesion of the coatings even without a base layer and the results are consistent with those reported in the literature [9-11].

The coating deposition time was programmed constant for all the three processes in order to limit the thickness in the range of 2 μm ; however slight variation in thickness were measured. The substrate bias of -65 V resulted in the thickest coating i.e. in the range of 2.13 μm , whereas -75 V and -95 V resulted in the range of 1.96 μm and 1.84 μm respectively. This thickness decrease can be attributed to the strong ion-bombardment resulting in re-sputtering of the deposited coating. Table 1 gives the characterisation results obtained for the coatings with various analytical techniques.

As evident from the results, coatings deposited at $U_{BIAS} = -95V$ exhibited the highest values of hardness (40 GPa) and residual stress of compressive nature (-10 GPa). As the substrate bias was reduced to lower values, hardness and compressive stress values also reduced. Hardness and stress values around 36 GPa and -7 GPa respectively were measured for $U_{BIAS} = -75 V$ deposited coatings and further reduced to 32 GPa and -5 GPa respectively for coatings deposited at $U_{BIAS} = -65 V$. The roughness values of the coatings, measured on Si specimens, however were near consistent in the range of 0.05 – 0.06 μm . All coatings also exhibited near consistent and low sliding wear coefficients in the range of $6 - 7 \times 10^{-15} m^3 N^{-1} m^{-1}$ suggesting high sliding wear resistance.

All the coatings exhibited an FCC NaCl structure as evident in the figure 3. The coatings deposited at $U_{BIAS} = -95 V$ exhibited a dominating 111 texture. Although the 111 orientation was the strongest for all bias voltages, contributions from other directions increased as the bias voltage was reduced to -75 V and with $U_{BIAS} = -65 V$ resulting in mixed orientation of the grains. The results indicate a strong influence of the ion bombardment energy on the texture in turn controlled by the bias voltage and consistent with the measured residual stress values of the coatings. EMPA studies on the $U_{BIAS} = -95 V$ coatings showed the coating composition to be near stoichiometric with N/ Zr atomic ratio of 1.11. Table 2.0 shows the spectrophoto analysis of the ZrN coatings. The results indicate that the coatings were of near consistent warm gold colour irrespective of the bias voltage, thus the coatings can be considered to be approximately of similar composition [12-13].

3.2: Microstructure analysis:

The effect of ion energy on the microstructure of the coatings was studied by X-TEM. Figure 4 shows the bright field (BF) TEM images of the coating. Figure 4(a) shows the top of the coating and figure 4(b) shows the whole coating cross-section deposited at $U_{BIAS} = -95$ V. These images indicate extremely dense microstructure of the coating. The column top (figure 4a) appears extremely flat and smooth. Figure 4b shows the full thickness cross-section. The coating appears to be densely packed with several grains oriented in the same direction or with a slight misorientation but difficult to resolve grain boundaries leading to the effect of a single column with large width; measuring in the range of 500 -700 nm. This is consistent with the strong texture of these coatings observed by x-ray diffraction studies presented in figure 3. This dense structure is in contrast to that often observed for processes such as magnetron sputtering or involving low ion bombardment; consisting of dome shaped column tops and easily resolved columnar grain boundaries (sometimes with voids) of the competitively grown columnar grains [14-17]. The large width of the columns can be attributed to the high ad-atom mobility caused by low energy ion bombardment achieved with HIPIMS. The effect of ion bombardment is notable provided only 2 magnetrons were being operated during deposition in a considerably large deposition chamber (volume of 1m^3) and with the target to substrate distance of 150 mm.

Figures 5 (a) and (b) show the coating deposited at $U_{BIAS} = -75$ V and -65 V respectively. As evident from the micrograph the coating microstructure appears extremely dense irrespective of the bias voltage with large grain diameters and hard to

resolve columnar grain boundaries. As evident from the images (figure 5a, b) the microstructures show mixed orientation which is in agreement with the XRD results (figure 3). The coating deposited with -65 bias volts (figure 5b) shows some portions of the coating top which resembles dome shape column, however on careful observation the peculiar dome top can be attributed to the changes in topography of the substrate (rough substrate morphology) and the coating following the contours of the substrate. Thus utilisation of HIPIMS results in extremely dense coating structures with smooth morphology. The smooth and macroparticle (arc droplets) and growth defects free (intercolumnar voids and under dense structures) morphology can be attributed to the increased ad-atom mobility and or re-sputtering effect due to the applied bias voltage to the substrates. These dense structures resemble the transition zone structures in the famous Structure Zone Diagrams (SZD) reported by Thornton for PVD coatings [18]. Dense coating microstructure with HIPIMS, however without substrate biasing (floating potentials), has also been reported in the literature [19].

Figure 6 shows the AFM images of the as-deposited surface of the coatings deposited on Si (100) substrates at 3 different bias voltages. As evident from the images, these coatings on the whole show near similar morphologies: dense and smooth, except for the variation in the z-axis value in the growth direction (representing the maximum height of a feature from the reference line; the reference line being the lowest point in the scan). Coatings deposited at $U_{BIAS} = -95$ V shows the least z-axis value thus suggesting very flat surface, -75 bias volts an intermediate value where as coating deposited at $U_{BIAS} = -65$ V is the roughest in the set (in agreement with the Ra values reported in table 1).

4. Conclusions:

Monolayer ZrN coatings were successfully deposited in an industrial sized PVD machine exclusively by the novel HIPIMS technique. A strong influence of the ion bombardment from the ionised deposition species on the microstructure of the coatings was observed.

(a) The results show extremely dense, columnar grain micro-structures of the coating, free of macro particle and under-dense structures irrespective of the deposition bias voltages.

(b) High bombardment of the depositing species with low energy ionised flux during growth of the coating promotes high ad-atom movement resulting in the growth of large diameter columnar grains. The structure is fully dense even with lower bias voltage ($U_{BIAS} = -65$ V) and is in contrast to those observed of 'V' shaped competitive growth often visible for low ionised processes such as sputtering.

(c) A strong 111 texture exists for coatings subjected to high bombardment ($U_{BIAS} = -95$ V) with increasing contributions from other directions as bias voltage is dropped to -75 V whereas for low bias voltage ($U_{BIAS} = -65$ V) the structure shows mixed orientation.

(d) ZrN coatings showed excellent adhesion (in excess of 100 N) and high hardness (range of 31 to 40 GPa) and superior microstructures resulting in high sliding wear resistance.

Acknowledgments: The authors would like to thank Ms. Christina Wuestefeld, Freiberg University, Germany for the EPMA measurements and Prof. W Mark Rainforth, Department of Engineering Materials, Sheffield University, UK for providing the transmission electron microscope facilities.

References

- [1] P.C. Johnson and H. Randhawa, Surf. Coat. Technol. 33 (1987) 53.
- [2] W.D. Sproul, Thin Solid Films 107 (2) (1983) 141.
- [3] C. Reinhard , A.P. Ehiasarian, P.Eh. Hovsepian, Thin Solid Films 515 (2007) 3685.
- [4] I. G. Brown, B. Feinberg, and J. E. Galvin, J. Appl. Phys. 63 (1988) 4889.
- [5] I. Petrov, P. Losbichler, D. Bergstrom, J.E. Greene, W.-. Münz, T. Hurkmans, T. Trinh, Thin Solid Films 302, 1-2 (1997) 179.
- [6] V. Kouznetsov, K. Maca'k, J. M. Schneider, U. Helmersson, I. Petrov, Surf. Coat. Technol. 122, 2–3 (1999) 290.
- [7] A. P. Ehiasarian, R. New, W.-D. Münz, L. Hultman, U. Helmersson, V. Kouznetsov, Vacuum 65, 2 (2002) 147.
- [8] Fultz Brent and Howe James M., Transmission Electron Microscopy and Diffraction of Materials, 3rd Edition, Chapter 7, Springer, Berlin Heidelberg, 2008.
- [9] A. P. Ehiasarian, P. Eh. Hovsepian, W.-D.Münz, , "A Combined Process Comprising Magnetic Field-Assisted, High-Power, Pulsed Cathode Sputtering and an Unbalanced Magnetron": US Pat. 7081186B2, 2005, EP 1 260 603 A2, DE 10124749, 21.05. 2001.

- [10] A. P. Ehiasarian, J. G. Wen, I. Petrov, *J. Appl. Phys.* 101 (2007) 054301.
- [11] Papken Eh. Hovsepian, Arutiun P. Ehiasarian, Yashodhan P. Purandare, Reinhold Braun, Ian M. Ross, *Plasma Process. Polym.* 6 (2009) S118.
- [12] A.J. Perry, M. Georgson, W.D. Sproul, *Thin Solid Films* 157, 2 (1988) 255.
- [13] M. Nose, M. Zhou, E. Honbo, M. Yokota, S. Saji, *Surf. Coat. Technol.* 142-144 (2001) 211.
- [14] P. Eh Hovsepian, D. B. Lewis, W.-D. Münz, *Surf. Coat. Technol.* 133–134 (2000), 166.
- [15] R. Machunze, A.P. Ehiasarian, F.D. Tichelaar, G.C.A.M. Janssen, *Thin Solid Films* 518 (2009) 1561.
- [16] Y. P. Purandare, A. P. Ehiasarian and P. Eh. Hovsepian, *J. Vac. Sci. Technol.* 26 (2) (2008) 288.
- [17] A.P. Ehiasariana, P.Eh. Hovsepian, L. Hultman, U. Helmersson, *Thin Solid Films* 457 (2004) 270.
- [18] J.A. Thornton, *J. Vac. Sci. Technol.* 11 (1974) 666.
- [19] A. P. Ehiasarian, W.-D. Münz, L. Hultman, U. Helmersson, I. Petrov, *Surf. Coat. Technol.* 163-164 (2003) 267.

List of Figure Captions

Figure 1: Schematic representation of the deposition machine with the arrangements of the magnetrons and substrate table.

Figure 2: (a) Cross-sectional Bright field TEM image of the coating-substrate interface of the $U_{\text{BIAS}} = -95$ V coating (b) BSE-SEM image of the scratch test conducted on $U_{\text{BIAS}} = -95$ V coated specimen.

Figure 3: Bragg-Brentano X-ray diffraction measurements recorded for the ZrN nitride coatings as a function of bias voltage.

Figure 4: (a) Bright field TEM image of the top of the coating deposited at $U_{\text{BIAS}} = -95$ V. (b) Cross-sectional view of the whole coating with the SAD pattern of the coating in the inset.

Figure 5: Bright field TEM images of the coatings (a) deposited at $U_{\text{BIAS}} = -75$ V (b) deposited at $U_{\text{BIAS}} = -65$ V.

Figure 6: AFM images of the as-deposited ZrN coatings showing the topography.

Figure 1: Schematic representation of the deposition machine with the arrangements of the magnetrons and substrate table.

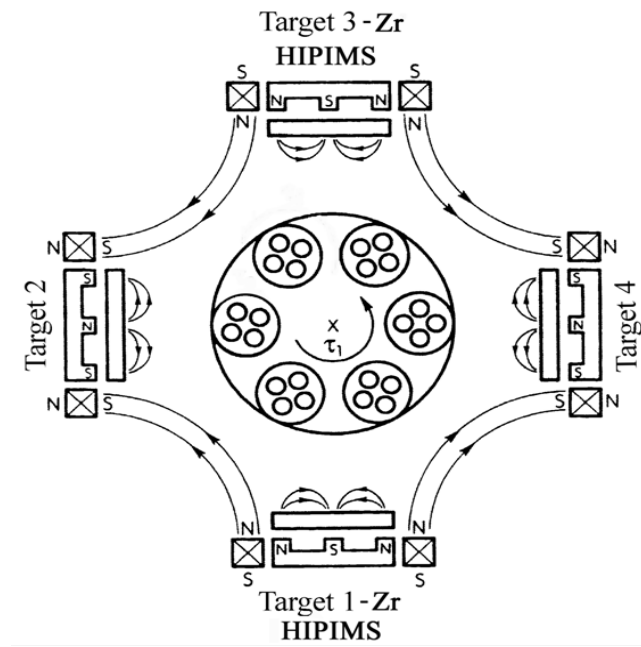


Figure 2: (a) Cross-sectional Bright field TEM image of the coating-substrate interface of the $U_{BIAS} = -95$ V coating (b) BSE-SEM image of the scratch test conducted on $U_{BIAS} = -95$ V coated specimen.

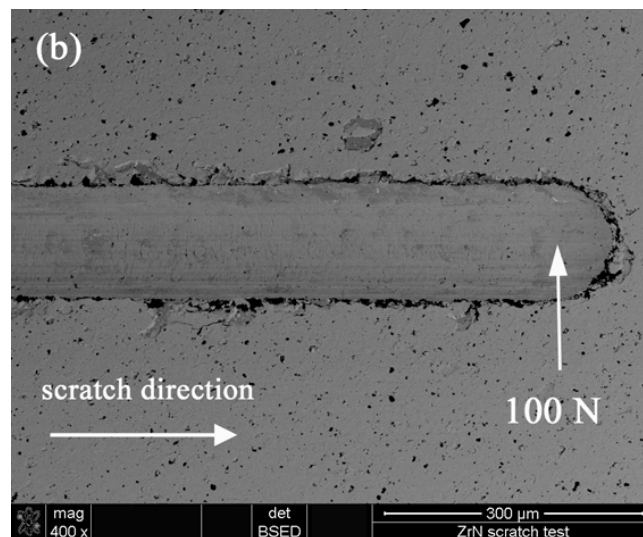
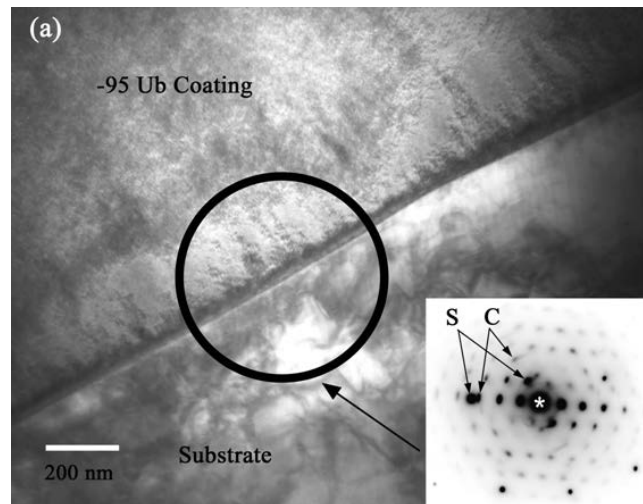


Figure 3: Bragg-Brentano X-ray diffraction measurements recorded for the ZrN nitride coatings as a function of bias voltage.

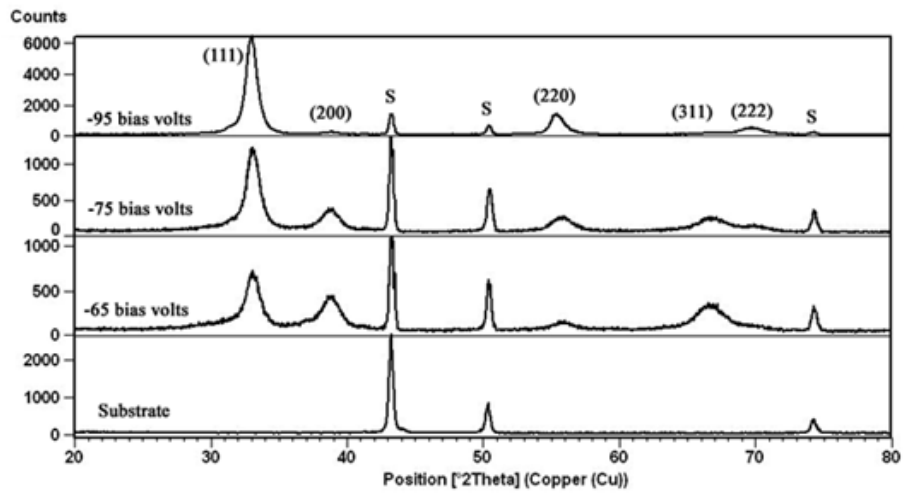


Figure 4: (a) Bright field TEM image of the top of the coating deposited at $U_{BIAS} = -95$ V. (b) Cross-sectional view of the whole coating with the SAD pattern of the coating in the inset.

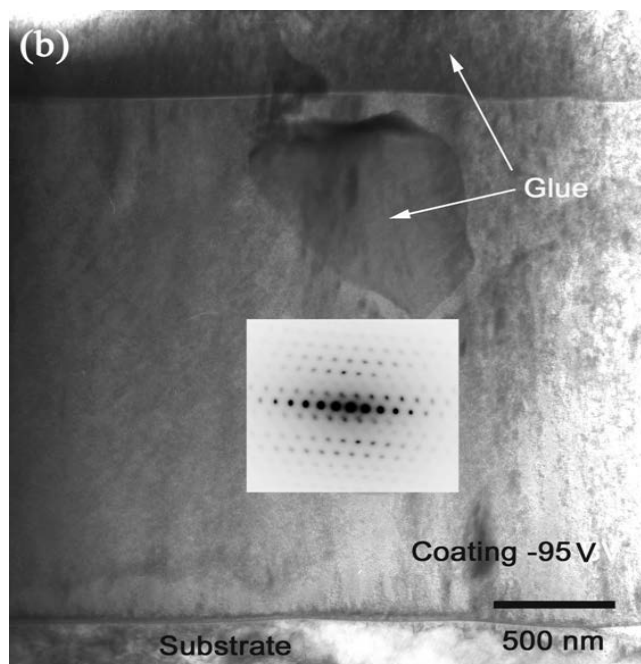
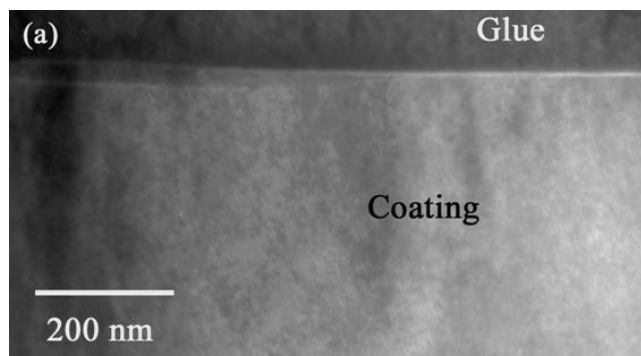


Figure 5: Bright field TEM images of the coatings (a) deposited at $U_{BIAS} = -75$ V (b) deposited at $U_{BIAS} = -65$ V.

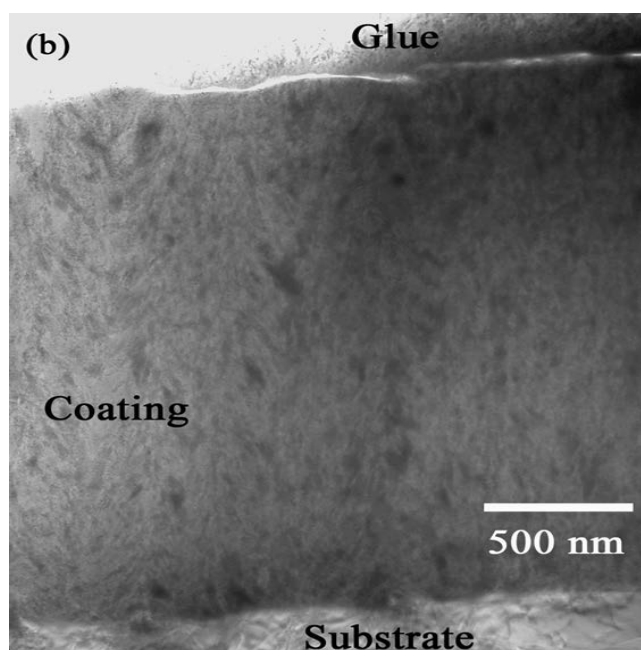
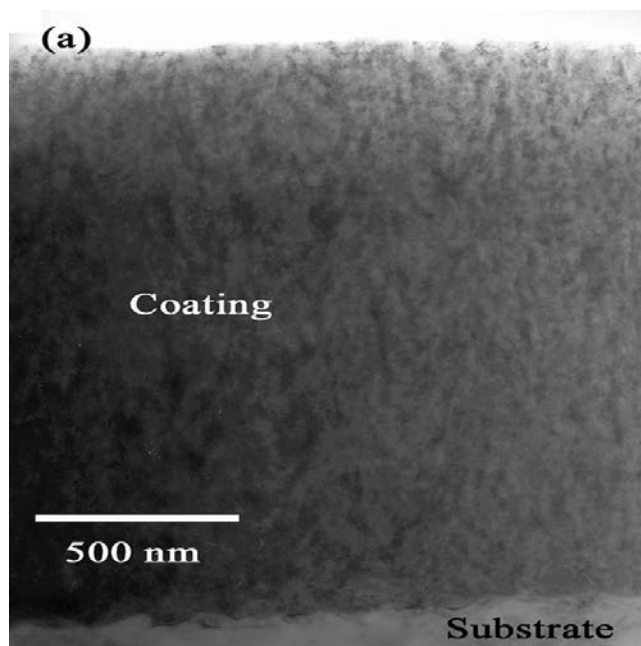
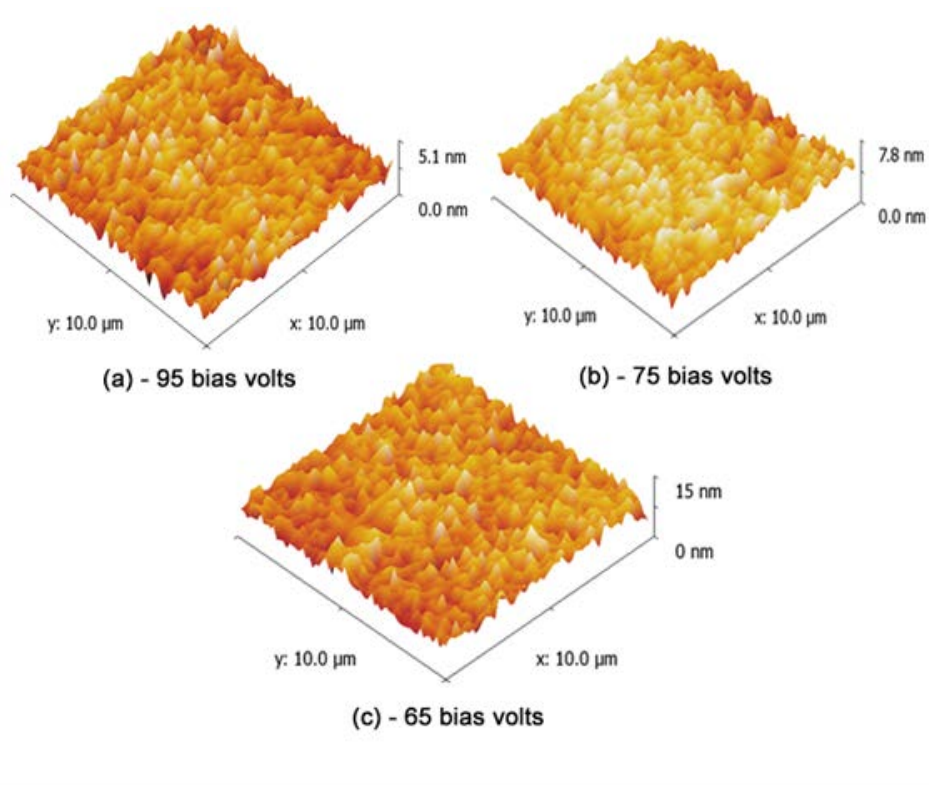


Figure 6: AFM images of the as-deposited ZrN coatings showing the topography.



List of Tables

Table I: Characterisation results measured for the ZrN coatings deposited at 3 different substrate bias voltages.

| Bias voltage | Nano-hardness (GPa) | Young's Modulus (GPa) | Adhesion (L_{C2}) | Stress (GPa) | Ra (μm) | Wear Coefficient, K_C ($\text{m}^3 \text{N}^{-1} \text{m}^{-1}$) | Thickness ($\mu\text{m}$) |
|---------------------|----------------------------|------------------------------|---------------------------------------|---------------------|--------------------------------------|---|---|
| -95 | 40.4 ± 3.2 | 424.4 | > 100 N | -10 ± 0.7 | 0.056 | 6.84×10^{-15} | 1.84 |
| -75 | 36.6 ± 3.6 | 358.5 | > 100 N | -7.7 ± 0.7 | 0.058 | 6.37×10^{-15} | 1.96 |
| -65 | 31.9 ± 7.7 | 370.8 | > 100 N | -5.1 ± 0.4 | 0.062 | 7.19×10^{-15} | 2.13 |

Table II: Colour measurements of the coatings recorded with a spectrophotometer.

| Bias voltage | L* | a* | b* |
|---------------------|-----------|-----------|-----------|
| -95 | 77.28 | 2.33 | 38.70 |
| -75 | 71.55 | 6.41 | 36.78 |
| -65 | 74.41 | 4.37 | 37.74 |